Physica B 591 (2020) 412261

Contents lists available at ScienceDirect

Physica B: Physics of Condensed Matter

journal homepage: http://www.elsevier.com/locate/physb

MoS_2 induced the enhancement of nonlinear absorption of Ag thin film

Zhengwang Li [a], Ruijin Hong [a,*], Qingyou Liu [b], Jing Liao [a], Qianbing Cheng [a], Qi Wang [a], Chunxian Tao [a], Hui Lin [a], Dawei Zhang [a]

[a] Engineering Research Center of Optical Instrument and System, Ministry of Education and Shanghai Key Lab of Modern Optical System, University of Shanghai for Science and Technology, No.516 Jungong Road, Shanghai, 200093, China
[b] Key Laboratory of High-temperature and High-pressure Study of the Earth's Interior, Institute of Geochemistry, Chinese Academy of Sciences, Guiyang, 550081, China

ARTICLE INFO

Keywords:
Ag/MoS_2 composite thin films
Z-scan measurement
Surface plasmon resonance
Nonlinear absorption response
Enhanced electric field

ABSTRACT

In this work, Ag/MoS_2 composite thin films were fabricated. The effects of MoS_2 layer on the structure and optical properties of Ag thin film were investigated. XRD results show that MoS_2 buffer layer has the effects of promoting grain growth of Ag and increasing their particle sizes confirmed by SEM images. The surface plasmon resonance (SPR) wavelength of Ag was observed to shift from 432 nm to 1650 nm with the introduction of MoS_2 buffer layer. The nonlinear absorption (NLA) response of Ag/MoS_2 composite thin films was significantly improved compared with that of the Ag single layer, which is attributed to the SPR of the Ag/MoS_2 composite thin films and the enhanced electric field induced by SPR. Moreover, the simulation results of Finite-Difference Time-Domain (FDTD) are in good agreement with the experimental results.

1. Introduction

The nonlinear optical (NLO) properties of nanomaterials play a key role in advanced photonic devices. Noble metal (Au, Ag, Cu) nanoparticles (NPs) have broad nonlinear optical applications such as optical modulators and optical switches [1–3]. Metal NPs own a strong light absorption coefficient caused by surface plasmon resonance (SPR). In SPR, the conductive electrons are collectively excited by a local electric field [4,5]. The increased effective NLO response can be realized by the plasmonic effect [6]. Plasmonic excitation can enhance nonlinear optical effects through many ways. First, the coupling of light and surface plasma will lead to a strong local electromagnetic field [7]. Second, plasmonic excitation is sensitive to the dielectric properties of metals and surrounding media [8]. Finally, plasmonic excitation can respond to several femtoseconds timescale, thus allowing ultra-fast processing of optical signals [9]. However, noble metal NPs can not be directly used in optical switching, optical limiting, and other fields. The unsatisfactory effect is limited by its nonlinear absorption (NLA) response is still not strong enough. Recently, the optical nonlinear enhancement caused by effective photon-photon interaction in Au–CdS [10], Ag–CdS [11], and Au–CdTe [12] has been reported. Hence, Composite thin films based on metal and semiconductor materials have potential applications in photonics and optoelectronics due to the high degree of optical nonlinear and ultra-fast time response [12–16].

At present, the transition metal dichalcogenides has attracted more and more interest in the next generation optoelectronic devices due to their excellent band structures [17,18]. For example, the saturated absorption and two-photon absorption of MoS_2 films have been widely studied. As discussed above, the excellent properties of metal-semiconductor films far exceed those of individual structures due to the tight coupling of metal elements and semiconductor counterparts [19]. In the metal-semiconductor films, the NLA response of the material can be enhanced by improving the SPR and the corresponding local field environment [20,21]. Therefore, MoS_2 may be a promising candidate for enhancing the nonlinear absorption of noble metal materials.

In this paper, we adopted MoS_2 as a buffer layer and fabricated Ag/MoS_2 using electron beam (EB) evaporation deposition technology. Moreover, we investigated the effects of MoS_2 buffer layer on the structure as well as optical properties of Ag thin film. The comparative NLA response of the MoS_2, Ag, and Ag/MoS_2 were investigated by using an ultra-fast laser with the same intensity at 1550 nm. Furthermore, FDTD results show that the Ag/MoS_2 composite thin films have stronger electric field intensity than that of MoS_2 or Ag single layer.

* Corresponding author.
E-mail address: rjhong@usst.edu.cn (R. Hong).

https://doi.org/10.1016/j.physb.2020.412261
Received 11 March 2020; Received in revised form 2 May 2020; Accepted 9 May 2020
Available online 12 May 2020

2. Experiment

2.1. Preparation

MoS_2 and Ag thin films were successively deposited by EB evaporation from MoS_2 and Ag target, respectively. The chamber pressure was 5.0×10^{-4} Pa. The thickness of MoS_2 and Ag thin films was 10 nm. For Ag/MoS_2 composite thin films, the thickness of both the inner layer MoS_2 and the outer layer Ag was 10 nm. The value of the thickness was monitored by quartz crystal microbalance which was placed in the evaporation chamber. The schematics of Ag, MoS_2, and Ag/MoS_2 structures are shown in Fig. 1(a–c).

2.2. Structural and optical characterization

The phases of these samples were characterized by XRD with CuKα radiation (λ = 0.15408 nm). The optical linear absorption of these samples was measured through a Perkins Elmer UV-VIS-NIR spectrophotometer. The surface morphology was investigated through SEM (merlincompact, ZEISS).

The third-order nonlinear optical property of these samples was characterized through the Z-scan system (T-Light, Menlosystems) whose excitation wavelength was 1550 nm. The Er-doped picosecond fiber laser delivers 2 ps pulses at 1550 nm and the repetition rate is 100 MHz. At present, the popular Z-scan technique is a method of focusing single beam, which measures the nonlinear absorption by translating the sample. In this work, these samples were moved above 30 mm through the waist of the laser beam. The sample undergoes maximum laser intensity at the focal point, and then decreases from either direction of the focal point. Fig. 1(d) is the Z-scan system.

3. Results and discussion

3.1. Optical characterization

Fig. 2 shows the SEM images of MoS_2, Ag and Ag/MoS_2 composite thin films, respectively. The single layer Ag thin film exhibit dewetting, consisting of microcone array particles with a diameter of about 2–4 μm. Compared to the single layer Ag thin film, Ag/MoS_2 composite thin films have larger Ag particle sizes about 8–10 μm, as shown in Fig. 2(c). The SEM images show that the introduction of a MoS_2 buffer layer is beneficial to the growth of Ag grains. The reason for the larger size of Ag particles is that the MoS_2 acts as a buffer layer on which metal can converge better [22]. Specifically, the surface free energy of metallic Ag is larger than that of oxide and MoS_2, so that thermal evaporation process causes shrinkage of Ag on the surface of K9 substrate and MoS_2 [23]. Ag better converge on MoS_2 is attributed to the fact that metal shrinkage on the substrates will be affected by a variety of factors, such as strain energy, the surface free energy, and diffusion activation energy between metal atoms and substrate surface [24]. Due to the higher strain energy, Ag film is easier to be shrunk on the MoS_2 buffer layer and form micro-particles.

XRD patterns as shown in Fig. 3(a) reveal the effect of MoS_2 buffer layer on the structure of Ag thin film. For single layer Ag thin film, there are several diffraction peaks at around 38.02°(2θ), 44.24°(2θ), 64.46°(2θ), and 77.3°(2θ), corresponding to (111), (200), (220), and (311) of Ag (JCPDS: 89-3722), respectively. The strongest diffraction peak at 38.02°(2θ) indicates the preferred orientation of Ag grains along (111) crystal plane. Mainly, for the non-epitaxial deposition, the surface tends to lie on (111) or (001) plane due to minimum surface free energies [25]. Compared with the powder Ag, the diffraction peak position of the single layer Ag film drifts, which is caused by the film stress. After the MoS_2 buffer layer is applied, the diffraction peak position further drifts, indicating that the stress is further increased. These peaks located at 25.74°(2θ) and 53.12°(2θ) correspond to (110) and (220) planes of Ag_2S (JCPDS: 76-0134), respectively. In the process of EB evaporation, slight amounts of Ag will react with MoS_2 to form Ag_2S and the consumption of Ag leads to the weakening of the XRD peak intensity of Ag in Ag/MoS_2 composite thin films. The diffraction peak at around 14.28°(2θ) corresponds to (002) of MoS_2 (JCPDS: 73-1508) is not observed, which is attributed to MoS_2 is covered by the Ag layer. Significantly, for pure MoS_2 thin film, the diffraction peak of the MoS_2 is relatively weak because its thickness is only 10 nm and the crystallinity is poor. Moreover, the broad big peak comes from the K9 substrate. The film thickness is thin and the structure is still in the discontinuous state, which leads to the high noise of XRD detection.

The optical absorption spectra obtained from Ag thin film with and without MoS_2 buffer layer are shown in Fig. 3(b). For Ag single layer, there is a slight SPR band around 432 nm. With the increase of wavelength, the absorption intensity decreases gradually. When the structure of Ag film is continuous, no obvious absorption peak will be observed. In other words, the discontinuous Ag film can produce strong resonance frequency and lead to an absorption peak [26]. The SEM images well confirmed the state of Ag particles in the samples. When MoS_2 buffer layer is applied, the absorption intensity of Ag/MoS_2 composite thin films is significantly enhanced as compared to that of the single Ag or MoS_2 layer. It should be noted that there is an obvious spectral characteristic near 448 nm corresponding to the c excition of MoS_2 [27]. Hence, in the UV-VIS region, the higher intensity of Ag/MoS_2 is caused by the proximity of MoS_2 c exciton to Ag SPR, in which there is enough peak overlap to cause intensity increasing [27]. In the NIR range, for Ag/MoS_2 composite thin films, the strong light absorption from 1200 nm to 2500 nm can be referred to as the SPR of Ag particles. Actually, due to the surface confinement, the size of metal particles limits the collective charge oscillations [28]. However, with the increase of the size, charge separation increases. Therefore, the collective electron oscillation needs a lower frequency, which can be seen from the red-shift of the plasma peak in the absorption spectra [29]. By adjusting the dimension of noble metal particles, the light absorption response induced by plasma resonance can be adjusted from the VIS region to the NIR region [30]. The introduction of MoS_2 buffer layer makes the Ag particles converge better and the size becomes larger, which results in the strong resonance absorption peak of the Ag/MoS_2 composite films in the NIR region and is consistent with the above analysis.

3.2. NLO properties

The third-order nonlinear absorption was measured by open aper-

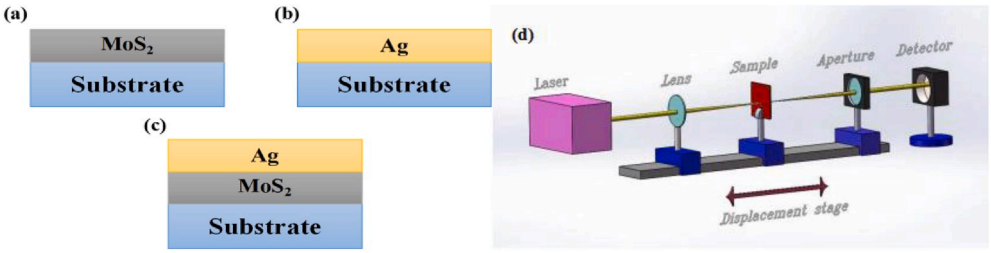

Fig. 1. Schemes of (a) MoS_2, (b) Ag, (c) Ag/MoS_2 composite thin films, and (d) Z-scan system.

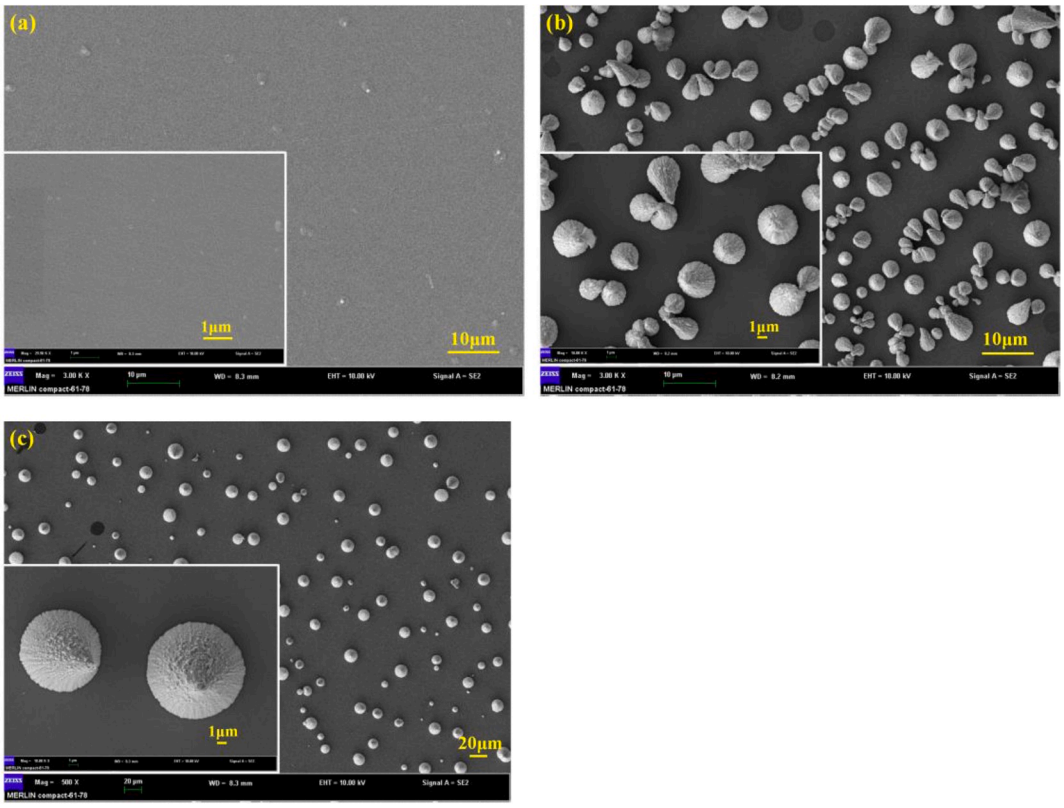

Fig. 2. SEM images of (a) MoS_2, (b) Ag, and (c) Ag/MoS_2 composite thin films.

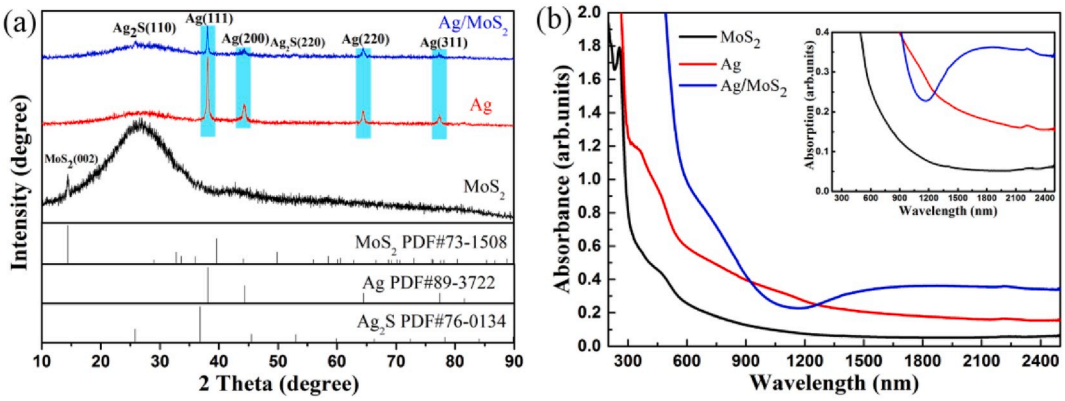

Fig. 3. (a)The XRD patterns of MoS_2, Ag, and Ag/MoS_2 composite thin films, (b)UV-VIS-NIR absorption spectra of MoS_2, Ag, and Ag/MoS_2 composite thin films.

ture Z-scan system with the excitation energy of 3.1×10^{-3} GW/cm^2 and the excitation wavelength is 1550 nm. The absorption of the sample under strong excitation can be described as:$\alpha(I) = \alpha_0 + \beta(I)I$, where α_0 and β are the linear and nonlinear absorption coefficient, respectively. Based on the NLO theory, equation $dI/dz' = -\alpha_0 I - \beta I^2$can quantitatively describe the propagation process of laser in samples, where I and z' represent the excitation intensity and propagation distance, respectively. All the normalized transmittance curves can be fitted theoretically as follows:

$$T(z) = \frac{\ln[1 + q_0(z)]}{q_0(z)} \quad (1)$$

Here, $q_0(z) = \beta(I_0 L_{eff})/(1 + z^2/z_0^2)$, $L_{eff} = [1 - e^{-\alpha_0 L}]/\alpha_0$, z is the longitudinal distance between the focal point (z = 0) and sample, z_0 is the diffraction length of beam, I_0 is the laser intensity at the waist, L_{eff} and L represent sample's effective path length and sample length, respectively.

These films exhibit NLA response under picosecond laser excitation as shown in Fig. 4. The blank substrate was tested by Z-scan and found that there was no nonlinear phenomenon to eliminate the influence of the blank substrate on the nonlinear of these samples. MoS_2 thin film exhibits slight reverse saturated absorption with the intensity of 0.27×10^{-3} GW/cm^2, while the Ag single layer shows obvious saturated absorption in Z-scan system, and the maximum normalized transmittance is 1.15. When MoS_2 buffer layer was applied, the transmittance exhibits a maximum at the focus (z = 0) with a value of 1.25. In other words, the single layer Ag thin film and Ag/MoS_2 composite thin films can inhibit the transmission of low-intensity light, but allow for the transmission of high-intensity light [31]. These results show that the saturated absorption of Ag/MoS_2 composite thin films is significantly higher than that of single Ag layer. According to the fitting results, the coefficient β is calculated as shown in Fig. 4(b). MoS_2 thin film exhibits slight reverse

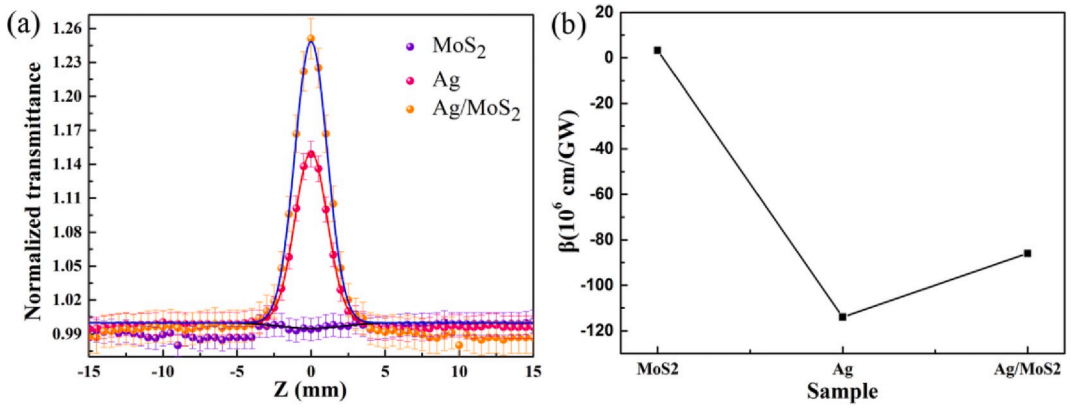

Fig. 4. (a) Open aperture Z-scan curves of MoS_2, Ag, and Ag/MoS_2 composite thin films, (b) the value of nonlinear absorption (β) of the samples.

saturated absorption behavior and consequently positive sign for β. Conversely, Ag and Ag/MoS_2 samples exhibit negative signs, and the value is -1.14×10^8 cm/GW and -8.6×10^7 cm/GW, respectively. Moreover, Ag/MoS_2 sample exhibits a low saturable intensity ($\sim 1.4 \times 10^{-3}$ GW/cm^2) compared with that of the Ag thin film ($\sim 1.6 \times 10^{-3}$ GW/cm^2). In short, the introduction of MoS_2 buffer layer is effective to enhance the NLO properties of single layer Ag thin film.

3.3. Nonlinear optical enhancement mechanism

Single layer Ag thin film shows saturated absorption characteristics, and the NLA coefficient β is negative. When Ag particles are excited by the laser with the wavelength of 1550 nm, charge transfer may occur between the s-band in the conductive band and the p-band, and finally, the s-conduction band is bleached at a lower intensity. Therefore, electrons can't move from the s-band to a higher level, and Ag particles show a high degree of transparency near the focal region [32]. For Ag/MoS_2 composite thin films, the NLA enhancement is mainly due to the introduction of MoS_2 buffer layer. The Ag film would be easier to be shrunk with higher strain energy on the MoS_2 buffer layer, forming micro-particles. The size of Ag particles increases and leads to the strong SPR in the NIR range [33], and the 1550 nm excitation is located near the peak of the SPR band of the Ag particles. The observed SA can be attributed to ground state plasma bleaching. The z-scan data show that the increase of excitation flux leads to the bleaching of ground state plasma absorption as the Ag/MoS_2 thin films move to the beam focus [34]. Concurrently, SPR with excellent light-trapping and electromagnetic field enhancement characteristics is propitious to the light absorption around metal particles [33]. In other words, the electric field enhancement effect induced by SPR will produce large nonlinear absorption at the SPR wavelength [35].

In order to explore the effect of the MoS_2 buffer layer on the electric field intensity of single layer Ag thin film, the finite element method was used to simulate the electric field distribution as shown in Fig. 5. Here, Fig. 5(a) represents the electric field distribution of MoS_2 continuous thin films, Fig. 5(b) and (c) represent the electric field distribution at the junction between Ag particle and the buffer layer (K9 substrate, MoS_2), respectively. The maximum joint electric field intensity enhancement factors of the samples with and without MoS_2 buffer layer are 3.1 and 1.9, respectively, which indicates a relatively strong SPR mode about Ag/MoS_2 composite thin films. The results of the simulation are consistent well with the NLA phenomena.

4. Conclusion

In summary, we investigated the effects of MoS_2 buffer layer on the crystal quality, composition, morphology, and optical properties of the Ag thin film. SEM images show that Ag particles can converge better on the surface of MoS_2 buffer layer and the size of the Ag particles in the Ag/MoS_2 composite thin films is 2.5–4 times larger than that of Ag single layer. The linear absorption spectra indicate the SPR wavelength of Ag particles can be tuned by the addition of MoS_2 layer. The NLA of MoS_2, Ag, and Ag/MoS_2 composite thin films were investigated, and the results show that MoS_2 layer is beneficial to enhance the nonlinear saturated absorption of Ag thin films, which is attributed to the SPR induced near the excitation wavelength of 1550 nm. The FDTD results show that there is a relatively strong SPR mode about Ag/MoS_2 composite thin films than that of single layer Ag thin film. This work provides a new idea for the engineering of NLA properties of metal-semiconductor structures, and can promote the development and application of nonlinear photonic devices based on plasmon.

Declaration of competing interest

We declare that we have no financial and personal relationships with other people or organizations that can inappropriately influence our

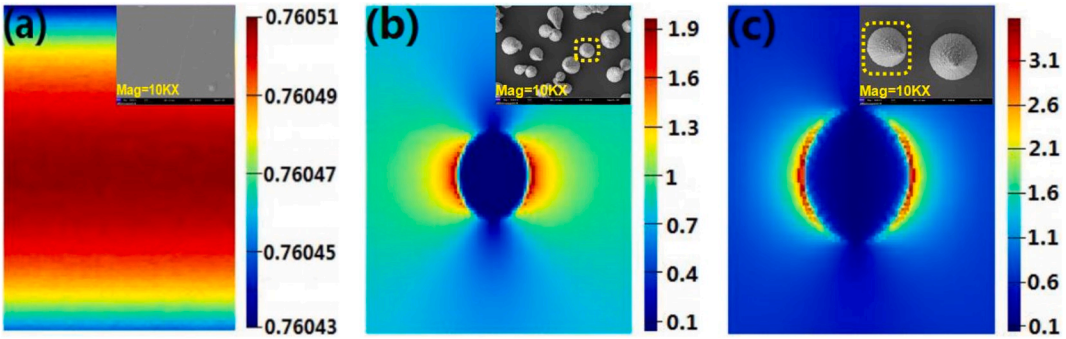

Fig. 5. Electric field distribution of (a) MoS_2, (b) Ag and (c) Ag/MoS_2 composite thin films.

work; there is no professional or other personal interest of any nature or kind in any product, service and/or company that could be construed as influencing the position presented in, or the review of, the manuscript entitled.

CRediT authorship contribution statement

Zhengwang Li: Writing - original draft. **Ruijin Hong:** Writing - review & editing, Supervision. **Qingyou Liu:** Investigation. **Jing Liao:** Software. **Qianbing Cheng:** Software. **Qi Wang:** Data curation. **Chunxian Tao:** Data curation, Formal analysis. **Hui Lin:** Project administration, Validation.

Acknowledgments

This work was supported by the National Natural Science Foundation of China (61775140, 61775141), and Shanghai Foundation for Science and Technology Innovation Action Plan (1714220060).

References

[1] Y. Zhang, S. Wang, H. Yu, H. Zhang, Y. Chen, L. Mei, A. Di Lieto, M. Tonelli, J. Wang, Sci. Rep. 5 (2015) 11342.
[2] Q. Guo, Y. Yao, Z. Luo, Z. Qin, G. Xie, M. Liu, J. Kang, S. Zhang, G. Bi, X. Liu, J. Qiu, ACS Nano 10 (2016) 9463–9469.
[3] S. Wang, Y. Zhang, R. Zhang, H. Yu, H. Zhang, Q. Xiong, Adv. Opt. Mater. 3 (2015) 1342–1348.
[4] B. Xu, L. Wang, Z. Ma, R. Zhang, Q. Chen, C. Lv, B. Han, X. Xiao, X. Zhang, Y. Zhang, K. Ueno, H. Misawa, H. Sun, ACS Nano 8 (2014) 6682–6692.
[5] A. Furube, L. Du, K. Hara, R. Katoh, M. Tachiya, J. Am. Chem. Soc. 129 (2007) 14852–14853.
[6] M. Kauranen, A.V. Zayats, Nat. Photon. 6 (2012) 737–748.
[7] A.V. Zayats, I.I. Smolyaninov, A.A. Maradudin, Phys. Rep. 408 (2005) 131–314.
[8] J. Homola, Chem. Rev. 108 (2008) 462–493.
[9] M.I. Stockman, Optic Express 19 (2011) 22029–22106.
[10] F. Nan, S. Liang, X. Liu, X. Peng, M. Li, Z. Yang, L. Zhou, Z. Hao, Q. Wang, Appl. Phys. Lett. 102 (2013) 163112.
[11] H. Gong, X. Wang, Y. Du, Q. Wang, J. Chem. Phys. 125 (2006) 24707.
[12] M. Fu, K. Wang, H. Long, G. Yang, P. Lu, F. Hetsch, A.S. Susha, A.L. Rogach, Appl. Phys. Lett. 100 (2012), 063117.
[13] M. Achermann, J. Phys. Chem. Lett. 1 (2010) 2837–2843.
[14] R. Costi, A.E. Saunders, E. Elmalem, A. Salant, U. Banin, Nano Lett. 8 (2008) 637–641.
[15] K.K. Haldar, S. Kundu, A. Patra, Appl. Phys. Lett. 104 (2014), 063110.
[16] N. Fan, S. Liang, X. Liu, X. Peng, M. Li, Z. Yang, L. Zhou, Z. Hao, Q. Wang, Appl. Phys. Lett. 102 (2013) 163112.
[17] Z. Sun, A. Martinez, F. Wang, Nat. Photon. 10 (2016) 227.
[18] Y. Xue, Y. Zhang, Y. Liu, H. Liu, J. Song, J. Sophia, J. Liu, Z. Xu, Q. Xu, Z. Wang, J. Zheng, Y. Liu, S. Li, Q. Bao, ACS Nano 10 (2015) 573.
[19] V. Sreeramulu, K.K. Haldar, A. Patra, D.N. Rao, J. Phys. Chem. C 118 (2014) 30333–30341.
[20] Y. Pu, R. Grange, C.L. Hsieh, D. Psaltis, Phys. Rev. Lett. 104 (2010) 207402.
[21] M.R. Singh, Nanotechnology 24 (2013) 125701.
[22] Z. Wang, L. Peng, Z. Lin, J. Ni, P. Yi, X. Lai, X. He, Z. Lei, Sci. Rep. 7 (2017) 13155.
[23] G. Yang, X. Fang, Y. Gu, N. Lu, X. Zhang, Y. Wang, B. Hua, X. Ni, Q. Fan, X. Gu, Appl. Surf. Sci. 508 (2020) 144794–144800.
[24] G. Yang, Y. Guo, H. Zhu, D. Yan, G. Li, S. Gao, K. Dong, Appl. Surf. Sci. 285P (2013) 772–777.
[25] R. Hong, X. Wang, J. Ji, C. Tao, D. Zhang, D. Zhang, Appl. Surf. Sci. 356 (2015) 701–706.
[26] R. Hong, W. Shao, W. Sun, C. Deng, C. Tao, D. Zhang, Opt. Mater. 77 (2018) 198–203.
[27] J.G. DiStefano, Y. Li, H.J. Jung, S. Hao, A.A. Murthy, X. Zhang, C. Wolverton, V. P. Dravid, Chem. Mater. 30 (2018) 4675–4682.
[28] W. Knoll, Annu. Rev. Phys. Chem. 49 (1998) 569–638.
[29] C.M. Cobley, M. Rycenga, F. Zhou, Z. Li, Y. Xia, Angew. Chem., Int. Ed. Engl. 48 (2009) 4824–4827.
[30] Q. Zhang, W. Li, C. Moran, J. Zeng, J. Chen, L. Wen, Y. Xia, J. Am. Chem. Soc. 132 (2010) 11372–11378.
[31] K. Wang, J. Wang, J. Fan, M. Lotya, A. O' Neill, D. Fox, Y. Feng, X. Zhang, B. Jiang, Q. Zhao, H. Zhang, J.N. Coleman, L. Zhang, W.J. Blau, ACS Nano 7 (2013) 9260–9267.
[32] R. Allu, D. Banerjee, R. Avasarala, S. Hamad, S.V. Rao, G.K. Podagatlapalli, Opt. Mater. 96 (2019) 109305.
[33] M. He, C. Quan, C. He, Y. Huang, L. Zhu, Z. Yao, S. Zhang, J. Bai, X. Xu, J. Phys. Chem. C 121 (2017) 27147–27153.
[34] C. Gao, W. Wu, D. Kong, L. Ran, Q. Chang, H. Ye, Physica E 45 (2012) 162–165.
[35] H. Dai, L. Zhang, Z. Wang, X. Wang, J. Zhang, H. Gong, J. Han, Y. Han, J. Phys. Chem. C 121 (2017) 12358–12364.